J. Biochem. **137**, 157–166 (2005)
DOI: 10.1093/jb/mvi015

Cleavage of Nonmuscle Myosin Heavy Chain-A during Apoptosis in Human Jurkat T Cells

Masahiko Kato*, Hiroyuki Fukuda, Takashi Nonaka† and Shinobu Imajoh-Ohmi‡

Department of Basic Medical Sciences, Institute of Medical Science, University of Tokyo, Minato-ku, Tokyo 108-8639

Received October 12, 2004; accepted November 19, 2004

We have previously reported that calpastatin, an endogenous inhibitory protein of calpain, is cleaved by a caspase-3–like protease during apoptosis in human Jurkat T cells [Kato, M. *et al.* (2000) *J. Biochem.* 127, 297–305]. In this study, we found that nonmuscle myosin heavy chain-A (NMHC-A) is cleaved during apoptosis in Jurkat cells by using a cleavage-site–directed antibody for calpastatin. The cleavage-site–directed antibody was raised against the amino-terminal fragment of calpastatin, and this antibody detected the *in vitro* cleaved calpastatin fragment. Although cleaved calpastatin was not detected, a 95-kDa polypeptide (p95) was detected in apoptotic cells by this antibody. This p95 was identified as the carboxyl-terminal fragment of NMHC-A based on the results of peptide mass spectrometry fingerprinting and amino-terminal sequencing. Furthermore, two cleavage sites on NMHC-A, Asp-1153 and Asp-1948, were determined, and three cleaved fragments of NMHC-A, one cleaved at Asp-1153 and the other two cleaved at Asp-1948, were detected by cleavage-site–directed antibodies against each cleavage site. The results of confocal immunofluorescence microscopic analysis show that the cleavage at Asp-1948 occurs faster than that at Asp-1153 during apoptosis. In addition, the Asp-1153 cleaved fragment was distributed diffusely in the cytoplasm of apoptotic cells, whereas the Asp-1948 cleaved fragments were detected as condensed dots. In conclusion, our findings can be summarized as follows: (i) NMHC-A is cleaved at two sites during apoptosis, (ii) the timing of cleavage is different between these two cleavage sites, and (iii) the distribution of cleaved fragments is different in apoptotic cells.

Key words: apoptosis, caspase, cleavage-site–directed antibody, nonmuscle myosin heavy chain-A, Jurkat T-cell.

Abbreviations: NMHC-A, nonmuscle myosin heavy chain-A; Ac-DEVD-CHO, acetyl-Asp-Glu-Val-Asp-aldehyde; Ac-YVKD-CHO, acetyl-Tyr-Val-Lys-Asp-aldehyde; PARP, poly (ADP-ribose) polymerase; PVDF, polyvinylidene fluoride; Z-Asp-CH_2-DCB, carbobenzoxy-Asp-[(2,6-dichlorobenzoyl) oxy] methane; Z-IEAL-CHO, carbobenzoxy-Ile-Glu (OtBu)-Ala-Leu-aldehyde; Z-VAD-fmk, carbobenzoxy-Val-Ala-Asp-fluoromethylketone; Z-LLL-CHO, carbobenzoxy-Leu-Leu-Leu-aldehyde; Z-LL-CHO, carbobenzoxy-Leu-Leu-aldehyde.

Apoptosis is a major form of physiological cell death that is critical to several biological processes and involves various intracellular proteolytic systems (*1–6*). Caspases play important roles in apoptosis-executing processes, since the inhibition of caspases results in the suppression of apoptosis (*7*, *8*). All known caspases are synthesized as inactive proenzymes containing a prodomain, and their activation results from cleavage (*9*). The active sites of caspases have a well conserved pentapeptide, QACXG (where X is Q, R, or G), and an absolute requirement for an aspartic acid residue at the P_1 position (*1*).

Among caspases, caspase-3 has been proposed to be a key enzymes for apoptosis, because apoptosis is prevented when caspase-3 activation is inhibited by a specific inhibitor (*10*). Caspase-3 preferentially recognizes DXXD sequences that are found in poly (ADP-ribose) polymerase (PARP) (*11*), DNA fragmentation factor 45 (ICAD) (*12*), and IκB-α (*13*). The cleavage of some substrates is closely related to apoptotic phenomena; degradation of ICAD results in the activation of DNase and the fragmentation of chromosomal DNA (*14*, *15*). Caspase-7 resembles caspase-3 in substrate specificity but displays different profiles with regard to intracellular redistribution in apoptosis (*16*, *17*).

Previously, we reported that calpastatin, an endogenous inhibitor protein of calpain, is cleaved by caspase-3 and/or caspase-7 during apoptosis in human Jurkat T cells (*18*). Subsequently, to analyze the cleaved fragment, we produced a cleavage-site–directed antibody (#1234) designed to react with the amino-terminal fragment of calpastatin. The cleavage-site–directed antibody is a very useful tool to analyze cleaved fragments because this type of antibody reacts with the new amino-terminal or carboxyl-terminal sequence that appears as a result of proteolysis (*19–21*). Unexpectedly, #1234 detected a 95-kDa polypeptide (p95) in apoptotic cells, although the

*Present address: Department of Biochemistry, Tokyo Women's Medical University, 8-1 Kawada-cho, Shinjuku-ku, Tokyo 162-8666.
†Present address: Department of Molecular Neurobiology, Tokyo Institute of Psychiatry, 2-1-8, Kamikitazawa, Setagaya-ku, Tokyo 156-8585.
‡To whom correspondence should be addressed. Tel: +81-3-5449-5311, Fax: +81-3-5449-5491, E-mail: ohmi@ims.u-tokyo.ac.jp

amino-terminal fragment of calpastatin was not detected. This p95 was identified as the carboxyl-terminal fragment of nonmuscle myosin heavy chain-A (NMHC-A). Myosin is a major cytoskeletal protein in eukaryotic cells and participates in various cellular processes including cell locomotion (*22–24*). Conventional myosins found in nonmuscle cells, referred to as nonmuscle myosin heavy chain (NMHC), arise from at least two genes, for NMHC-A and NMHC-B (*25*, *26*). Both isoforms are hexameric proteins comprising two heavy chains (approximately 200 kDa) and two pairs of light chains of 17 kDa and 20 kDa. NMHC includes a globular head domain and a rod-like tail domain. The globular head domain at the amino terminus associates with ATP, actin, and a pair of myosin light chains; whereas the rod-like tail domain at the carboxyl-terminal forms an α-helical coiled-coil and is concerned with the assembly of NMHC molecules into bipolar filaments (*27*). Additionally, the carboxyl-terminus of the rod-like tail has a short nonhelical tailpiece, which regulates the assembly of NMHC (*28*, *29*).

In this paper, we describe the cleavage of NMHC-A during apoptosis. Suarez-Huerta *et al.* have also reported that NMHC-A is cleaved during apoptosis (*30*). However, they did not determine the cleavage site. We determined two cleavage sites in NMHC-A. Furthermore, we confirmed the timing of cleavage at both these sites and the distribution of the cleaved fragments.

MATERIALS AND METHODS

Reagents—The following reagents were obtained from the following sources: carbobenzoxy-Val-Ala-Asp-fluoromethylketone (Z-VAD-fmk), Bachem (Switzerland); carbobenzoxy-Asp-[(2,6-dichlorobenzoyl) oxy] methane (Z-Asp-CH_2-DCB), acetyl-Tyr-Val-Lys-Asp-aldehyde (Ac-YVKD-CHO), acetyl-Asp-Glu-Val-Asp-aldehyde (Ac-DEVD-CHO), carbobenzoxy-Ile-Glu (OtBu)-Ala-Leu-aldehyde (Z-IEAL-CHO), carbobenzoxy-Leu-Leu-Leu-aldehyde (Z-LLL-CHO), and carbobenzoxy-Leu-Leu-aldehyde (Z-LL-CHO), Peptide Institute Inc. (Osaka, Japan); anti-nonmuscle myosin antibody, Biomedical Technologies Inc. (Stoughton, MA, USA).

Cell Culture and Induction of Apoptosis—Human T-lymphoblastoid Jurkat cells were maintained in RPMI1640 medium supplemented with 10% (v/v) fetal calf serum, 2 mM Gln, 100 U/ml penicillin G, and 200 μg/ml streptomycin at 37°C under a humidified atmosphere of 5% (v/v) CO_2. For the induction of apoptosis, the cells (10^6 cell/ml) were treated with 25 ng/ml anti-Fas mAb (MBL, Nagoya) and 0.5 μM staurosporine (Sigma Chemicals, St. Louis, MO, USA). For microscopic analysis, the cells were cytospun and stained with Carrazi's Hematoxylin, as described previously (*31*).

Immunoblotting—The following antibodies were raised in rabbits using synthetic peptides as haptens conjugated with a carrier protein and purified from antisera by affinity chromatography on immobilized antigen peptides. Anti-human cleaved calpastatin (#1234) was raised against residues 222–233 (SSKPIGPDDAID). Anti-NMHC-A cleaved the amino-terminal fragment (#1439) was raised against residues 1144–1153 (LKTELEDTLD). Anti-NMHC-A cleaved the carboxyl-terminal fragment (#1522) was raised against residues 1934–1948 (MARK-GAGDGSDEEVD). Anti-human PARP has been described previously (*18*).

The procedures used for immunoblotting have also been described previously (*18*). Immunoabsorption using synthetic peptides was performed as follows. The synthetic peptide (2 nmol) was incubated with the #1234 antibody for 4 h at 4°C. The peptide-antibody mixture was used as the first antibody for immunoblotting.

Purification of p95—Apoptotic Jurkat cells were harvested and suspended in lysis buffer [50 mM Tris-HCl (pH 7.5) containing 5 mM EDTA]. The cells were lysed by sonication, and the water-insoluble fraction was prepared by centrifugation at 15,000 × *g* for 20 min in the cold. The pellet was incubated in lysis buffer containing 2 M NaCl for 30 min at 37°C. After centrifugation, an equal volume of 2 M $(NH_4)_2SO_4$ was added to the supernatant, the mixture was applied to a Butyl-Toyopearl column (TOSOH, Tokyo), and eluted with a linear gradient of 1–0 M $(NH_4)_2SO_4$. Immunoblotting identified the p95-containing fractions.

Identification of p95—Purified p95 was subjected to 7.5% (w/v) acrylamide SDS–polyacrylamide gel electrophoresis (PAGE) and the bands were transferred onto a nitrocellulose membrane (Protran, Schleicher & Schuell). The p95-containing regions were detected by reversible staining and excised; the blotted proteins were then cleaved by lysyl endopeptidase (Wako, Osaka). The molecular weights of the peptide fragments were analyzed by matrix-assisted laser desorption ionization-time-of-flight (MALDI-TOF) mass spectrometry (Voyager-DE PRO, Applied Biosystems). The protein was identified using the peptide mass fingerprinting analysis software MS-Fit (http://prospector.ucsf.edu/ucsfhtml4.0/msfit.htm).

Amino-Terminal Sequencing—Purified p95 was subjected to SDS-PAGE and transferred onto a PVDF membrane. The proteins were stained with 0.1% (w/v) Coomassie Brilliant Blue R250 in methanol, and the bands were excised and analyzed on a Beckman LF3000 protein sequencer.

Confocal Immunofluorescence Microscopy—Non-apoptotic or apoptotic Jurkat cells were harvested and washed in phosphate-buffered saline (PBS). The cells were suspended in PBS and placed on poly-L-lysine coated cover glasses for 15 min, fixed in 4% (w/v) paraformaldehyde in PBS for 10 min at room temperature, washed twice for 5 min each in PBS, and permeabilized with 0.2% (w/v) Triton X-100 for 10 min. After fixation and permeabilization, nonspecific antibody binding was blocked by incubation in 3% (w/v) BSA in PBS for 30 min. The cells were incubated with the first antibodies for 1 h at 37°C, washed three times for 5 min each in Tris-buffered saline (TBS) containing 0.05% (w/v) Tween 20, and incubated with FITC-conjugated anti-rabbit secondary antibody for 1 h at room temperature. After incubation with the second antibody, the cells were incubated with propidium iodide (50 ng/ml) for 20 min at room temperature in order to stain the nuclear DNA. After the final wash in PBS, the cells were mounted in fluorescence mounting medium (Vector Lab. Inc. Burlingame, CA) and viewed using an MRC-1024 confocal laser microscope (Bio Rad).

Other Methods—The *in vitro* cleavage of calpastatin was described previously (*18*).

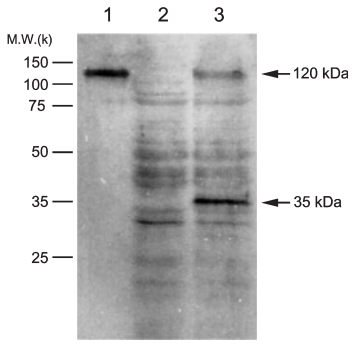

Fig. 1. ***In vitro* cleavage of calpastatin.** Recombinant calpastatin was incubated with the cytosol of Jurkat cells undergoing apoptosis. Unprocessed calpastatin (120 kDa) and its amino-terminal fragment (35 kDa) were stained by #1234 (arrows in figure). 1, recombinant calpastatin; 2, apoptotic cytosol without calpastatin; 3, calpastatin incubated with apoptotic cytosol.

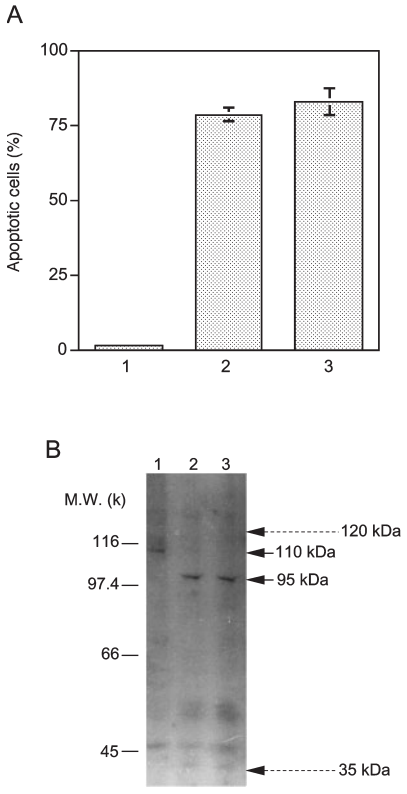

Fig. 2. **Immunoblotting using the #1234 antibody in non-apoptotic and apoptotic Jurkat cells.** Cells were treated with anti-Fas mAb or staurosporine for 24 h. A: Rate of apoptotic cells. Cells were mounted on a slide glass by cytocentrifugation and stained with Carrazi's Hematoxylin (Muto Pure Chemicals, Tokyo), as described previously (*27*). Nuclei were condensed into fragments and the cells were counted as apoptotic cells under a light microscopy. B: The immunoblot was stained with the #1234 antibody. Arrows with dotted lines indicate calpastatin (120 kDa) and its cleaved fragment (35 kDa), as shown in Fig. 1. 1, control cells without reagents; 2, anti-Fas mAb; and 3, staurosporine.

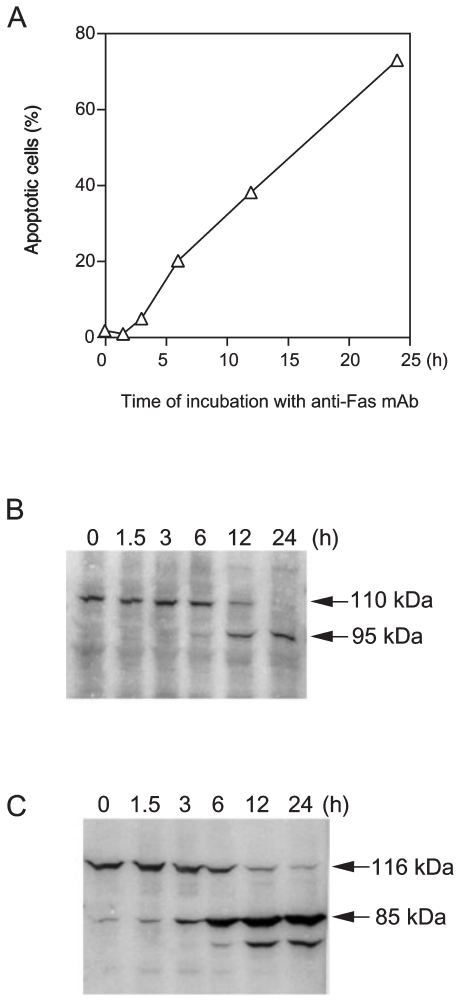

Fig. 3. **Appearance of p95 and disappearance of p110 during anti-Fas–mediated apoptosis.** Cells were treated with anti-Fas mAb and sampled for immunoblotting at the indicated times (0 to 24 h). A: Apoptotic cells were examined as described in the legend to Fig. 2. B: p110 and p95 were stained with the #1234 antibody (arrows). C: PARP (116 kDa) and its caspase-catalyzed fragment (85 kDa) stained with a PARP antibody.

RESULTS

The 95-kDa Polypeptide Was Detected by a Cleavage-Site–Directed Antibody in Apoptotic Jurkat Cells—Previously, we reported that calpastatin (120 kDa on SDS-PAGE) is cleaved to 90 kDa by caspase-3 and/or caspase-7 during apoptosis in Jurkat cell (*18*). The cleaved 90-kDa fragment was detected by an anti-calpastatin antibody against the carboxyl-terminal region of human calpastatin. Subsequently, we produced a cleavage-site-directed antibody (#1234) to analyze the cleaved amino-terminal fragment of calpastatin with an expected molecular mass of approximately 30 kDa. The #1234 antibody detected both unprocessed calpastatin (120 kDa) and the 35-kDa fragment when calpastatin was mixed with apoptotic cytosol (Fig. 1, lanes 1 and 3). The 35-kDa fragment is the amino-terminal polypeptide of calpastatin produced by caspase-3 and/or caspase-7, because this fragment was not observed in the apoptotic cytosol (Fig. 1,

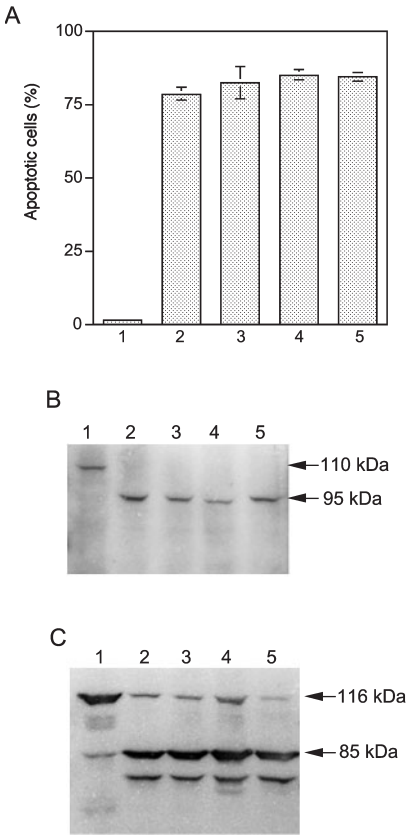

Fig. 4. **Effect of inhibitors of proteasome and calpain on the behavior of p110 and p95.** After pretreatment with inhibitors for 2 h, the cells were treated with anti-Fas mAb for 24 h. Apoptotic cells (A), the behavior of p110 and p95 (B), and the cleavage of PARP (C) were examined as described in the legend to Fig. 2. 1, control cells without mAb. Inhibitors added were: 2, none; 3, 50 μM Z-IEAL-CHO; 4, 100 μM Z-LLL-CHO; and 5, 100 μM Z-LL-CHO.

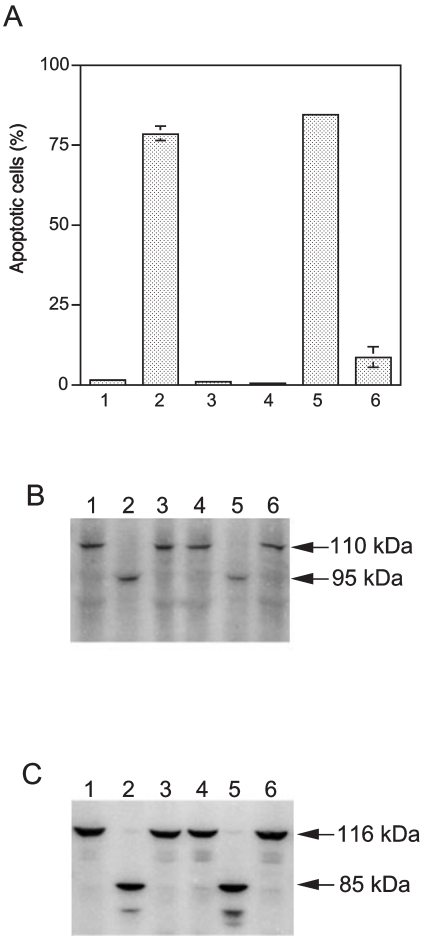

Fig. 5. **Effect of caspase inhibitors on the behavior of p110 and p95.** Cells were pretreated with caspase inhibitors for 2 h and further incubated with anti-Fas mAb for 24 h. Apoptotic cells (A), the behavior of p110 and p95 (B), and the cleavage of PARP (C) were examined as described in the legend to Fig. 2. 1, control cells without mAb. Inhibitors (100 μM) added were: 2, none; 3, Z-Asp-CH_2-DCB; 4, Z-VAD-fmk; 5, Ac-YVKD-CHO; and 6, Ac-DEVD-CHO.

lane 2). Next, we attempted to detect the cleaved amino-terminal calpastatin fragment in apoptotic Jurkat cells. Calpastatin was not detected by the #1234 antibody in non-apoptotic Jurkat cells; however, a protein with a molecular mass of 110 kDa (p110) on SDS-PAGE was observed (Fig. 2, lane 1). In anti-Fas mAb–induced apoptotic cells, neither calpastatin nor the 35-kDa fragment were detected (Fig. 2, lane 2). Although p110 had disappeared in the apoptotic cells, a 95-kDa polypeptide (p95), which had a larger molecular mass than the cleaved 90-kDa calpastatin fragment, was detected (Fig. 2, lane 2). The same phenomenon was observed in staurosporine induced apoptotic cells; staurosporine is an inhibitor of protein kinase C (Fig. 2, lane 3). The p95 polypeptide appeared after treatment with anti-Fas mAb for 6 h, while the level of p110 decreased after 12 h, and was hardly detected at 24 h (Fig. 3A). We also examined the proteolysis of poly (ADP-ribose) polymerase (PARP), a nuclear target for caspase-3 and/or caspase-7, which cleave PARP at Asp-214. This cleavage results in the generation of a 30-kDa DNA-binding amino-terminal and an 85-kDa catalytic carboxyl-terminal fragment. As shown in panels A and B in Fig. 3, the appearance of p95 occurred in parallel with the cleavage of PARP.

To determine whether the appearance of p95 and the disappearance of p110 were mediated by proteolysis during apoptosis, we examined the effects of various protease inhibitors. Inhibitors of proteasome, Z-IEAL-CHO and Z-LLL-CHO, and the inhibitor of calpain, Z-LL-CHO, did not inhibit the Fas-mediated apoptosis of Jurkat cells (Fig. 4A). None of these inhibitors affected the behavior of p95, p110, or the proteolysis of PARP during apoptosis (Fig. 4, B and C). Subsequently, we investigated the effects of inhibitors of various caspases on apoptosis and the behavior of p95 and p110 (Fig. 5). Z-Asp-CH_2-DCB and Z-VAD-fmk, caspase inhibitors with broad specificities, completely suppressed apoptosis, the appearance of p95 and the disappearance of p110, and the proteolysis of PARP. Ac-DEVD-CHO, which inhibits caspase-3 and caspase-7, also suppressed apoptosis, the appearance of p95 and the disappearance of p110, and the proteolysis of PARP. However, Ac-YVKD-CHO, which prefers caspase-1 and is less effective in the Fas-mediated apoptosis of Jurkat cells, did not inhibit the appearance of p95 and the disappearance of p110.

A

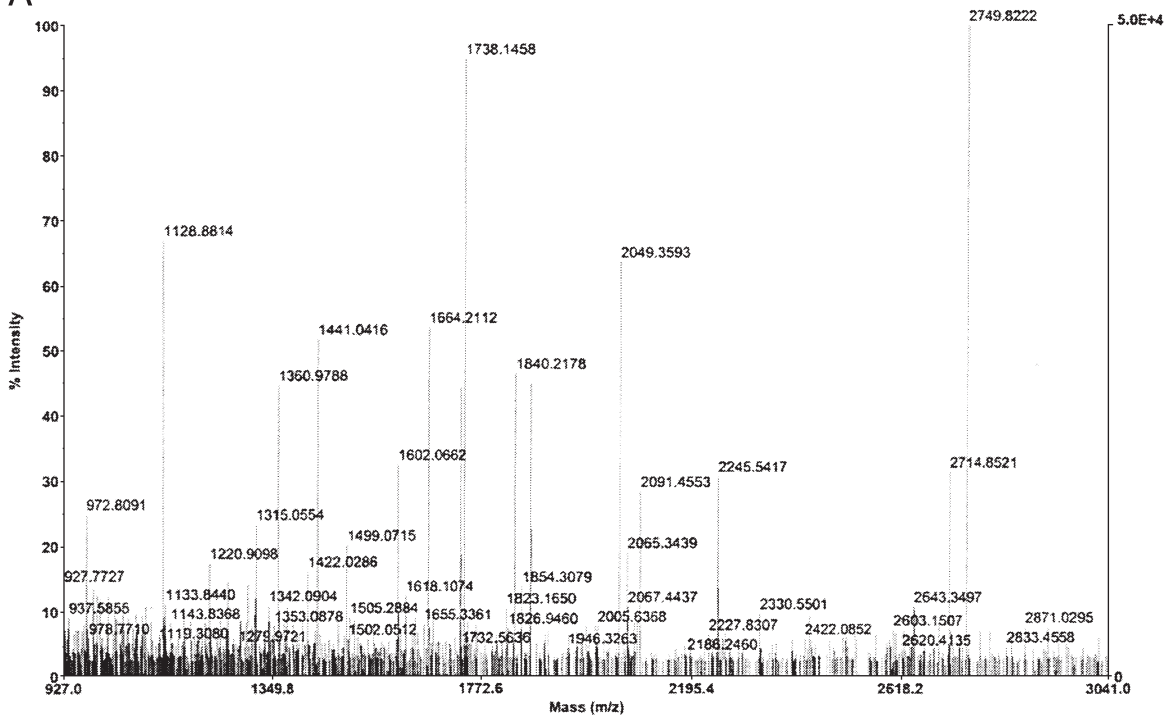

B

MAQQAADKYLYVDKNFINNPLAQADWAAKKLVWVPSDKSGFEPASLKEEVGEEAIVELVENGKKVKVNKD
DIQKMNPPKFSKVEDMAELTCLNEASVLHNLKERYYSGLIYTYSGLFCVVINPYKNLPIYSEEIVEMYKG
KKRHEMPPHIYAITDTAYRSMMQDREDQSILCTGESGAGKTENTKKVIQYLAYVASSHKSKKDQGELERQ
LLQANPILEAFGNAKTVKNDNSSRFGKFIRINFDVNGYIVGANIETYLLEKSRAIRQAKEERTFHIFYYL
LSGAGEHLKTDLLLEPYNKYRFLSNGHVTIPGQQDKDMFQETMEAMRIMGIPEEEQMGLLRVISGVLQLG
NIVFKKERNTDQASMPDNTAAQKVSHLLGINVTDFTRGILTPRIKVGRDYVQKAQTKEQADFAIEALAKA
TYERMFRWLVLRINKALDKTKRQGASFIGILDIAGFEIFDLNSFEQLCINYTNEKLQQLFNHTMFILEQE
EYQREGIEWNFIDFGLDLQPCIDLIEKPAGPPGILALLDEECWFPKATDKSFVEKVMQEQGTHPKFQKPK
QLKDKADFCIIHYAGKVDYKADEWLMKNMDPLNDNIATLLHQSSDKFVSELWKDVDRIIGLDQVAGMSET
ALPGAFKTRKGMFRTVGQLYKEQLAKLMATLRNTNPNFVRCIIPNHEKKAGKLDPHLVLDQLRCNGVLEG
IRICRQGFPNRVVFQEFRQRYEILTPNSIPKGFMDGKQACVLMIKALELDSNLYRIGQSKVFFRAGVLAH
LEEERDLKITDVIIGFQACCRGYLARKAFAKRQQQLTAMKVLQRNCAAYLKLRNWQWWRLFTKVKPLLQV
SRQEEEMMAKEEELVKVREKQLAAENRLTEMETLQSQLMAEKLQLQEQLQAETELCAEAEELRARLTAKK
QELEEICHDLEARVEEEEERCQHLQAEKKKMQQNIQELEEQLEEEESARQKLQLEKVTTEAKLKKLEEEQ
IILEDQNCKLAKEKKLLEDRIAEFTTNLTEEEEKSKSLAKLKNKHEAMITDLEERLRREEKQRQELEKTR
RKLEGDSTDLSDQIAELQAQIAELKMQLAKKEEELQAALARVEEEAAQKNMALKKIRELESQISELQEDL
ESERASRNKAEKQKRDLGEELEALKTELEDTLDSTAAQQELRSKREQEVNILKKTLEEEAKTHEAQIQEM
RQKHSQAVEELAEQLEQTKRVKANLEKAKQTLENERGELANEVKVLLQGKGDSEHKRKKVEAQLQELQVK
FNEGERVRTELADKVTKLQVELDNVTGLLSQSDSKSSKLTKDFSALESQLQDTQELLQEENRQKLSLSTK
LKQVEDEKNSFREQLEEEEEAKHNLEKQIATLHAQVADMKKKMEDSVGCLETAEEVKRKLQKDLEGLSQR
HEEKVAAYDKLEKTKTRLQQELDDLLVDLDHQRQSACNLEKKQKKFDQLLAEEKTISAKYAEERDRAEAE
ARETKETKALSLARALEEAMEQKAELERLNKQFRTEMEDLMSSKDDVGKSVHELEKSKRALEQQVEEMKTQ
LEELEDELQATEDAKLRLEVNLQAMKAQFERDLQGRDEQSEEKKKQLVRQVREMEAELEDERKQRSMAVA
ARKKLEMDLKDLEAHIDSANKNRDEAIKQLRKLQAQMKDCMRELDDTRASREEILAQAKENEKKLKSMEA
EMIQLQEELAAAERAKRQAQQERDELADEIANSSGKGALALEEKRRLEARIAQLEEELEEEQGNTELIND
RLKKANLQIDQINTDLNLERSHAQKNENARQQLERQNKELKVKLQEMEGTVKSKYKASITALEAKIAQLE
EQLDNETKERQAACKQVRRTEKKLKDVLLQVDDERRNAEQYKDQADKASTRLKQLKRQLEEAEEEAQRAN
ASRRKLQRELEDATETADAMNREVSSLKNKLRRGDLPFVVPRRMARKGAGDGSDEEVDGKADGAEAKPAE

Fig. 6. **Identification of p95 by peptide mass spectrometry fingerprinting.** Purified p95 was digested with lysyl endopeptidase as described in "MATERIALS AND METHODS." The molecular mass of the derived peptides was measured by MALDI-TOF mass spectrometry. A, Mass fingerprinting of p95. B, Amino acid sequence of nonmuscle myosin heavy chain-A (NMHC-A). The peptides on which fingerprinting was performed are indicated by the red-letters.

Identification of p95—p95 was detected by #1234 in apoptotic cells but not in non-apoptotic cells. We believe that p95 was produced by proteolysis during apoptosis because 1234 is a cleavage-site–directed antibody that is designed to react with the carboxyl-terminal region of a cleaved amino-terminal calpastatin fragment. Subsequently, we attempted to identify the p95 fragment. To identify p95, we purified it from apoptotic Jurkat cells. It was observed that p95 was localized in the water-insoluble fraction of apoptotic cells. Additionally, p95 was not

Table 1. **Amino-terminal sequencing of p95.**

Amino-terminal sequence	Identification in NMHC-A
STAAQQELRS	$DTLD_{1153}$*STAAQQELRS

recovered by ultracentrifugation (100,000 × *g* for 60 min at 4°C) following treatment with 0.1% (w/v) Triton X-100 (data not shown). After several purification steps, as described in "MATERIALS AND METHODS," p95 was purified to an extent to which it could be excised as a single band on SDS-PAGE and subjected to lysyl endopeptidase digestion. The resulting peptides were analyzed by MALDI-TOF mass spectrometry (Fig. 6A), and a protein database search revealed that p95 is identical to nonmuscle myosin heavy chain-A (NMHC-A) (NCBI accession P35579). Figure 6B shows identical peptides located in the carboxyl-terminal region of NMHC-A. Furthermore, as shown in Table 1, the amino-terminal sequence of p95 is STAAQQELRS, indicating that NMHC-A is cleaved at Asp-1153.

Determination of the Cleavage Site in the Carboxyl-Terminal Region of NMHC-A—From the results of peptide mass fingerprinting analysis and amino-terminal sequencing, p95 was identified as the carboxyl-terminal fragment of NMHC-A. We considered that p95 would be cleaved in its carboxyl-terminal region, and that this polypeptide would have an aspartic acid residue at the end of the carboxyl-terminus, because #1234 was designed to react with the carboxyl-terminal region of the cleaved amino-terminal calpastatin fragment. We then investigated the epitope of #1234 to determine the cleavage site in the carboxyl-terminal of p95, because the epitope of #1234 coincides with the cleavage site. To determine the epitope of #1234, we performed immunoabsorption using synthetic peptides from the carboxyl-terminal region of NMHC-A, as described in "MATERIALS AND METHODS." We suspected that the carboxyl-terminal region of NMHC-A was cleaved by caspase because p95 was detected in apoptotic cells. First, we considered that the carboxyl-terminal region of NMHC-A was cleaved by caspase-3 and/or caspase-7. p95 contains three caspase-3/-7 consensus motifs, $DLKD_{1621}$ (peptide A in Fig. 7A), $DQAD_{1866}$ (peptide B), and $DGSD_{1944}$ (peptide C); however, these peptides did not inhibit the detection of p95 by #1234 (Fig. 7B, peptides A–C). Next, we synthesized six peptides derived from the carboxyl-terminal region from Asp_{1902} to Asp_{1952} (peptides D–I in Fig. 7A). To assess the inhibition of binding between #1234 and p95, one peptide comprising residues 1939–1948 of NMHC-A inhibited the detection of p95 by #1234 (Fig. 7, A and B, peptide H).

Detection of Three Cleaved NMHC-A Fragments in Apoptotic Cells—The results of amino-terminal sequencing and immunoabsorption analysis showed that during apoptosis, NMHC-A was cleaved at two sites, Asp-1153, and Asp-1948. To detect the cleaved NMHC-A fragments, two cleavage-site–directed antibodies were raised against the amino-terminal cleavage site (#1439) and the carboxyl-terminal cleavage site (#1522). A commercially available anti-nonmuscle myosin antibody detected a 205-kDa protein, presumably related to unprocessed NMHC-A in non-apoptotic cells, and also detected 204-kDa and 95-kDa polypeptides in apoptotic cells (Fig. 8A).

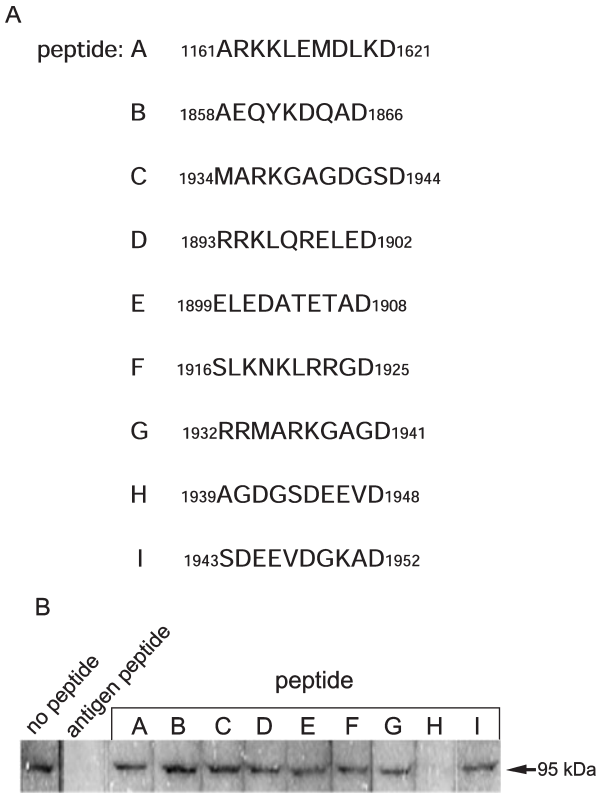

Fig. 7. **Immunoabsorption of #1234 using synthetic peptides derived from NMHC-A.** Synthetic peptides derived from the carboxyl-terminal region of NMHC-A were incubated with #1234 for 4 h at 4°C. A, Amino acid sequences of the synthetic peptides. Residue numbers are aligned with NMHC-A. B, Immunoblotting was performed using a peptide-antibody complex as the first antibody.

#1439 did not detect any proteins in non-apoptotic cells, but detected a 125-kDa fragment (p125) in apoptotic cells (Fig. 8B). Additionally, #1522 did not detect any proteins in non-apoptotic cells, whereas it detected both 204-kDa (p204) and 95-kDa (p95) fragments in apoptotic cells (Fig. 8C). The schematic representation of NMHC-A, including the cleavage sites and antibody recognition regions, are presented in Fig. 8D. Next, we examined the cleaved NMHC-A fragments using confocal immunofluorescence microscopy. We recognized four apoptotic phases depending on the staining pattern of the nuclear DNA by propidium iodide as follows: (i) non-apoptotic phase (Fig. 9, panels a, e, and i), (ii) early apoptotic phase (slight nuclear DNA condensation) (panel b, f, and j), (iii) nuclear DNA condensed phase (nuclear DNA completely condensed at the perinuclear region) (panels c, g, and k), and (iv) nuclear fragmented phase (panels d, h, and l). NMHC-A, detected by an anti-nonmuscle myosin antibody, was seen to be distributed diffusely in the non-apoptotic phase (Fig. 9, panel a); however, the distribution changed to condensed dots in the nuclear fragmented phase (panel d). The amino-terminal fragment of NMHC-A (p125), detected by #1439, was not observed in the non-apoptotic and early apoptotic phases (Fig. 9, panels e and f); however, it was detected diffusely in the cytoplasm in both the nuclear DNA condensed and the nuclear fragmented phases (panels g and h). Furthermore, the carboxyl-ter-

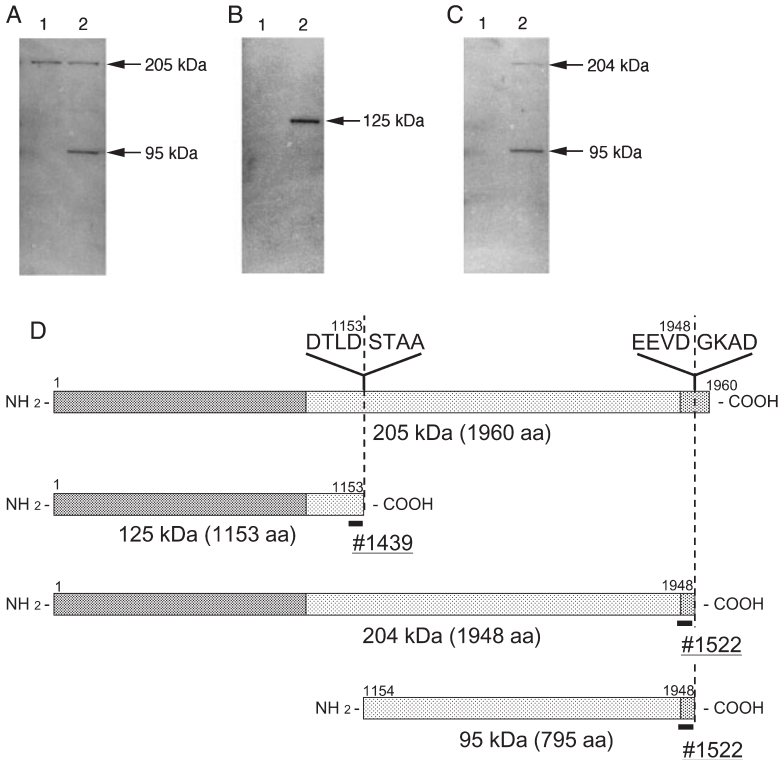

Fig. 8. **Defining cleaved NMHC-A fragments by using cleavage-site–directed antibodies.** Cells were treated with staurosporine for 12 h and sampled for immunoblotting. Staining during immunoblotting was performed using an anti-nonmuscle myosin antibody (panel A), #1439 raised against residues 1143–1153 of NMHC-A (B), and #1522 raised against residues 1934–1948 of NMHC-A (C). 1, control cells without staurosporine; 2, apoptotic cells. Arrows show unprocessed NMHC-A (205 kDa in panel A), the amino-terminal fragment (125 kDa in B), and the carboxyl-terminal cleaved fragments (204 kDa and 95 kDa in A and C). D: Schematic structure of NMHC-A. NMHC-A consists of globular head domain (dark gray) , rod-like tail domain (light gray), and nonhelical tailpiece (gray). Cleavage sites are indicated and the lengths of the cleaved fragments are shown in panels B and C are expressed as molecular mass on SDS-PAGE as well as residue number. The epitope regions of #1349 and #1522 are indicated by bold bars.

minal cleaved fragments (p204 and p95) detected by #1522 were not observed in the non-apoptotic phase (Fig. 9, panel i). However, these fragments were detected diffusely in the early apoptotic and nuclear DNA condensed phases (panels j and k), and detected as condensed dots in the nuclear fragmented phase (panel l). In the nuclear fragmented phase, similar staining patterns were observed when both the anti–nonmuscle myosin antibody and #1522 were used.

DISCUSSION

Cells undergoing apoptosis show diagnostic morphological features that include the condensation of chromatin, membrane blebbing, cell shrinkage, and cellular fragmentation. It has been reported that various cytoskeletal proteins, such as α-fodrin (*32*), gelsolin (*33*), β-catenin (*34*), vimentin (*30*, *35*), and actin (*36*), are cleaved by caspases, and that the proteolysis of these proteins induces the morphological changes that occur during apoptosis (*33*, *35*, *36*). In this study, we found that nonmuscle myosin heavy chain-A (NMHC-A), a cytoskeletal protein, is cleaved during apoptosis in human Jurkat T cells. Myosin is a hexametric protein that consists of two heavy chain subunits, two alkaline light chain subunits, and two regulatory light chain subunits (*27*). Cellular myosin appears to play a role in cytokinesis, stress fiber pulling, maintenance of the cortical actin layer, and secretion of vesicles (*37*, *38*).

We have already reported that calpastatin is cleaved during apoptosis (*18*). This cleavage is mediated by caspase-3 and/or caspase-7 and produces a 90-kDa fragment that can be detected by an antibody raised against the carboxyl-terminal region of calpastatin. In this study, we produced a cleavage-site–directed antibody (#1234) designed to detect the cleaved amino-terminal fragment of calpastatin with an expected molecular mass of approximately 30 kDa. This antibody detected an *in vitro* cleaved amino-terminal fragment of calpastatin (35 kDa), but not in apoptotic Jurkat cells. It has been reported previously that the amount of the 90-kDa calpastatin fragment is lower than expected from the reduction in molecular mass; this fragment probably undergoes further degradation by some as yet unidentified proteases (*18*). The amino-terminal fragment might also undergo further degradation similar to the 90-kDa fragment.

In this study, we unexpectedly detected a 95-kDa polypeptide (p95) using #1234 in apoptotic cells, and this p95 was identified as the carboxyl-terminal fragment of NMHC-A by peptide mass spectrometry analysis and amino-terminal sequencing. In addition, we determined the presence of two cleavage sites in NMHC-A. The first, Asp-1153, was determined by amino-terminal sequencing, which showed that p95 is generated by cleavage after the P_1 aspartic acid residue, $DTLD_{1153}$/S. The other cleavage site is Asp-1948. Since the cleavage-site–directed antibody is designed to react with either a newly appearing amino-terminal region or a carboxyl-terminal region (*19*), the epitope of this type of antibody coincides with the cleavage site. Based on this theory, we determined the cleavage site at Asp-1948 in NMHC-A by immunoabsorption using synthetic peptides, the results of which showed that p95 is produced by cleavage after the P1 aspartic acid residue $EEVD_{1948}$/G. Cleavage at both Asp-1153 and at Asp-1948 must be mediated by caspase(s) because pan-caspase inhibitors, but not other protease inhibitors, prevented the appearance of p95 *in vivo*, and all known caspases cleave after P_1 aspartic acid residues

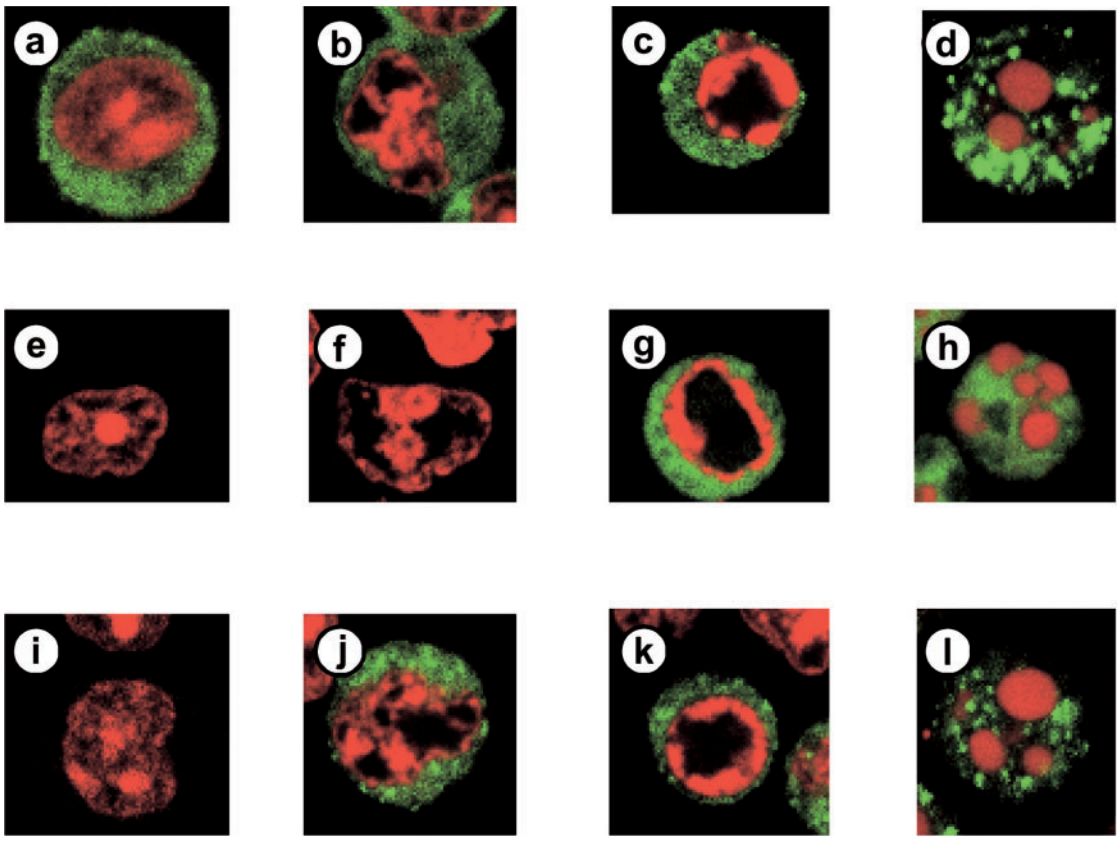

Fig. 9. **Detection of cleaved NMHC-A fragments by confocal immunofluorescence microscopy.** Staurosporine treated cells were fixed as described in "MATERIALS AND METHODS" and prepared for confocal immunofluoresence microscopy using anti–nonmuscle myosin antibody (panels a, b, c, and d), #1439 (e, f, g, and h), and #1522 (i, j, k, and l), respectively. Cells were double labeled with propidium iodide, which binds to nuclear DNA. Antibody staining is shown in green and nuclear DNA staining in red. The apoptotic phase was classified into groups depending on the staining pattern of nuclear DNA as follows: non-apoptptic phase (panels a, e, and i), early apoptotic phase (b, f, and j), nuclear DNA condensed phase (c, g, and k), and nuclear fragmented phase (d, h, and l).

(*1*). Among caspases, caspase-3 and/or caspase-7 could mediate the cleavage of NMHC-A, since the appearance of p95 was inhibited by the caspase-3/-7 specific inhibitor, Ac-DEVD-CHO. Between the two cleavage sites in NMHC-A, $DTLD_{1153}$/S fits the caspase-3/-7 consensus motif, DXXD, while $EEVD_{1948}$/G does not. Crystal structure analyses of the caspase-3 complex with the tetrapeptide inhibitor Ac-DEVD-CHO or Ac-DVAD-fluoromethylketone show that the P_4 aspartic acid side chain is enveloped in a narrow pocket that can accommodate small acidic or hydrophilic side chains (*39*, *40*). On the basis of these crystal structure analyses, caspase-3, and possibly caspase-7, might recognize the glutamic acid residue in the P_4 position instead of the aspartic acid residue. We attempted to construct a recombinant NMHC-A to determine whether caspase-3/-7 cleaves NMHC-A at the two identified cleavage sites; however, we were unable to obtain the cDNA of NMHC-A by RT-PCR from Jurkat RNAs.

The results of immunoabsorption indicate that #1234 reacts with the carboxyl-terminal sequence, EEVD-COOH, of p95. #1234 was raised against the carboxyl-terminal region of the cleaved amino-terminal calpastatin fragment. The carboxyl-terminal sequence of the antigen peptide is DAID-COOH. Comparing these carboxyl-terminal sequences, the P_1 aspartic acid residue can be identified. In addition, the P_2 residues, valine in p95 and isoleucine in the antigen, are classified into the hydrophobic amino acid group, and the P_4 residues, glutamic acid in p95 and aspartic acid in the antigen, are classified into the acidic amino acid group. Although the P_3 residues are classified into different amino acid groups, #1234 was able to cross react with the carboxyl-terminal sequence in p95 because the P_1, P_2, and P_4 residues in p95 and the antigen peptide are classified into the same amino acid groups.

As shown in Fig. 8, we detected three cleaved NMHC-A fragments using two cleavage-site–directed antibodies, #1439 and #1522, against each cleavage site; the amino-terminal fragment of NMHC-A was detected as a 125 kDa fragment (p125) by #1439, whereas the carboxyl-terminal cleaved fragments were detected as a 204 kDa fragment (p204) and a 95 kDa fragment (p95) by #1522. Furthermore, we also detected these cleaved NMHC-A fragments by confocal immunofluorescence microscopy using #1439 and #1522, respectively. The results of confocal imaging indicate that the cleavage at Asp-1948 occurred faster than that at Asp-1153 because the amino-terminal fragment was detected by #1439 in the nuclear DNA condensed phase, while the carboxyl-terminal cleaved fragments were detected by #1522 in the early apoptotic phase. NMHC-A contains two domains, a globular head domain at the amino-terminus, and a rod-like

tail domain in the carboxyl-terminal region. The globular head domain associates with actin, ATP, and myosin light chains, whereas the rod-like tail domain has no binding motifs; however, this domain contains a 28-residue repeat pattern composed of four heptapeptides, which is a characteristic of α-helical coiled-coils (*41*). Moreover, the rod-like tail domain has a short nonhelical sequence, referred to as a nonhelical tailpiece, at the carboxyl-terminus, and this nonhelical tailpiece regulates myosin assembly (*28*, *29*). On the basis of these reports, NMHC-A might disassemble and/or change from a dimer conformation by cleavage at Asp-1948 because one cleavage site, Asp-1948, exists in the nonhelical tailpiece. Subsequently, the other cleavage site, Asp-1153, would be exposed on the molecular surface by the cleavage of the nonhelical tailpiece; then, protease(s) such as caspase(s) could cleave at Asp-1153. In addition, as shown in Fig. 9, although the amino-terminal fragment was distributed diffusely, the carboxyl-terminal cleaved fragments were detected as condensed dots in the nuclear fragmented phase. These results suggest that the distribution of cleaved fragments is different in apoptotic cells. It has previously been reported that the overexpression of an amino-terminal region-deleted NMHC-A mutant induces cell rounding with rearrangement of actin filaments in HeLa cells (*42*). In rounding cells, the deleted mutant colocalizes with native NMHC-A, and the condensed dots appear similar to those observed in our results. p95 consists of a rod-like tail domain that forms α-helical coiled-coils, and this fragment could easily self-assemble under physiological conditions (*29*). From these findings, we conclude that the carboxyl-terminal cleaved fragments, p204 and p95, could aggregate. As a result of this aggregation, we observed condensed dots in the nuclear fragmented phase cell. On the other hand, the amino-terminal fragment, p125, was distributed diffusely in the cytoplasm. Since p125 contains a globular head domain, unlike p95, this domain can not self-assemble. In this case, p125 would distribute diffusely in apoptotic cells. In addition, we obtained the same staining patterns using an anti-nonmuscle myosin antibody and #1522 in the nuclear fragmented phase. Although we do not know the epitope of the anti-nonmuscle myosin antibody, it could react with the rod-like tail domain in NMHC-A because it detects p95 but not p125 in apoptotic cells, as shown in Fig. 8. We obtained the same results with both an anti-nonmuscle myosin antibody and #1522 when the anti-nonmuscle myosin antibody reacted with the rod-like tail domain.

Suarez-Huerta *et al*. also reported the cleavage of NMHC-A in bovine aortic endothelial cells during apoptosis (*30*). They detected the cleaved NMHC-A fragment (97 kDa) in 2D-PAGE and identified it by partial amino-terminal sequencing. This 97-kDa fragment is similar to the p95 found in this study, because the authors mentioned that all amino acid sequences obtained by partial amino-terminal sequencing are located in the carboxyl-terminal region of NMHC-A. Although Suarez-Huerta *et al*. reported NMHC-A cleavage during apoptosis, they did not observe the cleaved amino-terminal fragment. Furthermore, they were unable to determine the cleavage sites in NMHC-A. However, NMHC-A cleavage must be a general phenomenon during apoptosis because the results of Suarez-Huerta *et al*. and those of this study are similar with regard to NMHC-A cleavage in different types of cells. We have presented new findings about NMHC-A cleavage during apoptosis.

Figure 3 shows the 110-kDa protein (p110) detected by #1234 in non-apoptotic Jurkat cells, and this protein was not detected in apoptotic cells. Since the appearance of p95 occurs in parallel with the disappearance of p110, we first estimated that p110 could produce p95 by proteolysis during apoptosis. However, p110 was identified as an ATP and peptide-binding protein in germ cells-2 (Apg-2) (*43*) (data not shown). The carboxyl-terminus of Apg-2 is EMDID-COOH, whose sequence resembles that of the #1234 antigen peptide; #1234 could then cross-react with this protein. Apg-2 is a member of the heat shock protein (Hsp) 110 family and is expressed in all tissues including leukocytes (*43*). It has been reported that Hsp 70 is an effective inhibitor of apoptosis and exerts its anti-apoptotic function downstream of caspase-3 (*44*, *45*). Furthermore, Hsp 27 also inhibits apoptosis to prevent cytochrome *c*-dependent caspase-9 activation (*46*). Based on these reports, Apg-2 is probably concerned with apoptosis. However, the mechanism of the disappearance of Apg-2 during apoptosis is unknown.

Finally, we discuss the biological significance of NMHC-A cleavage during apoptosis. As noted earlier, cellular myosin has been implicated in various cellular processes. In apoptosis, myosin appears to be concerned with membrane blebbing, because the inhibition of the myosin motor activity prevents bleb formation (*47*). Furthermore, cell rounding with actin filament rearrangement is induced by the overexpression of the carboxyl-terminal region of NMHC-A (*42*). Various cytoskeletal proteins are cleaved during apoptosis, and these cleavages will contribute to the diagnostic morphological features of apoptosis. Based on these results, myosin is also implicated in the apoptotic morphological changes, and the cleavage of NMHC-A appears to be an important factor for morphological change during apoptosis.

We thank Nozomi Ichikawa for technical assistance in the peptide synthesis.

REFERENCES

1. Cohen, G.M. (1997) Caspases: the executioners of apoptosis. *Biochem. J.* **326**, 1–16
2. Ruiz-Vela, A., González de Buitrago, G., and Martinez-A, C. (1999) Implication of calpain in caspase activation during B cell clonal deletion. *EMBO J.* **18**, 4988–4998
3. Kikuchi, H., and Imajoh-Ohmi, S. (1995) Activation and possible involvement of calpain, a calcium-activated cysteine protease, in down-regulation of apoptosis of human monoblast U937 cells. *Cell Death Differ.* **2**, 195–199
4. Orlowski, R.Z. (1999) The role of the ubiquitin-proteasome pathway in apoptosis. *Cell Death Differ.* **6**, 303–313
5. Nakagawa, T. and Yuan, J. (2000) Cross-talk between two cysteine protease families. Activation of caspase-12 by calpain in apoptosis. *J. Cell Biol.* **150**, 887–894
6. Johnson, D.E. (2000) Noncaspase proteases in apoptosis. *Leukemia* **14**, 1695–1703
7. Thornberry, N.A. and Lazebnik, Y. (1998) Caspases: enemies within. *Science* **281**, 1312–1316
8. Shi, Y. (2004) Caspase activation: revisiting the induced proximity model. *Cell* **117**, 855–858

9. Hu, S., Snipas, S.J., Vincenz, C., Salvesen, G., and Dixit, V.M. (1998) Caspase-14 is a novel developmentally regulated protease. *J. Biol. Chem.* **273**, 29648–29653
10. Nicholson, D.W., Ali, A., Thornberry, N.A., Vaillancourt, J.P., Ding, C.K., Gallant, M., Gareau, Y., Griffin, P.R., Labelle, M., Lazebnik, Y.A., Munday, N.A., Raju, S.M., Smulson, M.E., Yamin, T., Yu, V.L., and Miller, D.K. (1995) Identification and inhibition of the ICE/CED-3 protease necessary for mammalian apoptosis. *Nature* **376**, 37–43
11. Lazebnik, Y.A., Kaufmann, S.H., Desnoyers, S., Poirier, G.G., and Earnshaw, W.C. (1994) Cleavage of poly (ADP-ribose) polymerase by a proteinase with properties like ICE. *Nature* **371**, 346–347
12. Enari, M., Sakahira, H., Yokoyama, H., Okawa, K., Iwamatsu, A., and Nagata, S. (1998) A caspase-activated DNase that degrades DNA during apoptosis, and its inhibitor ICAD. *Nature* **391**, 43–50
13. Barkett, M., Xue, D., Horvitz, H.R., and Gilmore, T.D. (1997) Phosphorylation of IκB-α inhibits its cleavage by caspase CPP32 *in vitro*. *J. Biol. Chem.* **272**, 29419–29422
14. Liu, X., Zou, H., Slaughter, C., and Wang, X. (1997) DFF, a heterodimeric protein that functions downstream of caspase-3 to trigger DNA fragmentation during apoptosis. *Cell* **89**, 175–184
15. Tang, D. and Kidd, V.J. (1998) Cleavage of DFF-45/ICAD by multiple caspases is essential for its function during apoptosis. *J. Biol. Chem.* **273**, 28549–28552
16. Jones, R.A., Johnson, V.L., Buck, N.R., Dobrota, M., Hinton, R.H., Chow, S.C., and Kass, G.E. (1998) Fas-mediated apoptosis in mouse hepatocytes involves the processing and activation of caspases. *Hepatology* **27**, 1632–1642
17. Chandler, J.M., Cohen, G.M., and MacFarlane, M. (1998) Different subcellular distribution of caspase-3 and caspase-7 following Fas-induced apoptosis in mouse liver. *J. Biol. Chem.* **273**, 10815–10818
18. Kato, M., Nonaka, T., Maki, M., Kikuchi, H., and Imajoh-Ohmi, S. (2000) Caspases cleave the amino-terminal calpain inhibitory unit of calpastatin during apoptosis in human Jurkat T cells. *J. Biochem.* **127**, 297–305
19. Kikuchi, H. and Imajoh-Ohmi, S. (1995) Antibodies specific for proteolyzed forms of protein kinase C α *Biochim. Biophys. Acta* **1269**, 253–259
20. Niikura, Y., Nonaka, T., and Imajoh-Ohmi, S. (2002) Monitoring of caspase-8/FLICE processing and activation upon Fas stimulation with novel antibodies directed against a cleavage site for caspase-8 and its substrate, FLICE-like inhibitory protein (FLIP). *J. Biochem.* **132**, 53–62
21. Iizuka, R., Chiba, K., and Imajoh-Ohmi, S. (2003) A novel approach for the detection of proteolytically activated transglutaminase 1 in epidermis using cleavage site-directed antibodies. *J. Invest. Dermatol.* **121**, 457–464
22. Lauffenburger, D.A., and Horwitz, A.F. (1996) Cell migration: a physically integrated molecular process. *Cell* **84**, 359–369
23. Fishkind, D.J. and Wang, Y.L. (1995) New horizons for cytokinesis. *Curr. Opin. Cell Biol.* **7**, 23–31
24. Young, P.E., Richman, A.M., Ketchum, A.S., and Kiehart, D.P. (1993) Morphogenesis in drosophila requires nonmuscle myosin heavy chain function. *Genes Dev.* **7**, 29–41
25. Katsuragawa, Y., Yanagisawa, M., Inoue, A., and Masaki, T. (1989) Two distinct nonmuscle myosin-heavy-chain mRNAs are differentially expressed in various chicken tissues. Identification of a novel gene family of vertebrate non-sarcomeric myosin heavy chains. *Eur. J. Biochem.* **184**, 611–616
26. Kawamoto, S. and Adelstein, R.S. (1991) Chicken nonmuscle myosin heavy chains: differential expression of two mrnas and evidence for two different polypeptides. *J. Cell Biol.* **112**, 915–924
27. Harrington, W.F. and Rodgers, M.E. (1984) Myosin. *Annu. Rev. Biochem.* **53**, 35–73
28. Murakami, N., Kotula, L., and Hwang, Y.W. (2000) Two distinct mechanisms for regulation of nonmuscle myosin assembly via the heavy chain: phosphorylation for MIIB and Mts 1 binding for MIIA. *Biochemistry* **39**, 11441–11451
29. Hodge, T.P., Cross, R., and Kendrick-Jones, J. (1992) Role of the COOH-terminal nonhelical tailpiece in the assembly of a vertebrate nonmuscle myosin rod. *J. Cell Biol.* **118**, 1085–1095
30. Suarez-Huerta, N., Lecocq, R., Mosselmans, R., Galand, P., Dumont, J.E., and Robaye, B. (2000) Myosin heavy chain degradation during apoptosis in endothelial cells. *Cell Prolif.* **33**, 101–114
31. Imajoh-Ohmi, S., Kawaguchi, T., Sugiyama, S., Tanaka, K., Omura, S., and Kikuchi, H. (1995) Lactacystin, a specific inhibitor of the proteasome, induces apoptosis in human monoblast U937 cells. *Biochem. Biophys. Res. Commun.* **217**, 1070–1077
32. Cryns, V.L., Bergeron, L., Zhu, H., Li, H., and Yuan, J. (1996) Specific cleavage of α-fodrin during Fas- and tumor necrosis factor- induced apoptosis is mediated by an interleukin-1β-converting enzyme/Ced-3 protease distinct from the poly (ADP-ribose) polymerase protease. *J. Biol. Chem.* **271**, 31277–31282
33. Kothakota, S., Azuma, T., Reinhard, C., Klippel, A., Tang, J., Chu, K., McGarry, T.J., Kirschner, M.W., Koths, K., Kwiatkowski, D.J., and Williams, L.T. (1997) Caspase-3-generated fragment of gelsolin: effector of morphological change in apoptosis. *Science* **278**, 294–298
34. Brancolini, C., Lazarevic, D., Rodriguez, J., and Schneider, C. (1997) Dismantling cell-cell contacts during apoptosis is coupled to a caspase- dependent proteolytic cleavage of β-catenin. *J. Cell Biol.* **139**, 759–771
35. Morishima, N. (1999) Changes in nuclear morphology during apoptosis correlate with vimentin cleavage by different caspases located either upstream or downstream of Bcl-2 action. *Genes Cells* **4**, 401–414
36. Mashima, T., Naito, M., and Tsuruo, T. (1999) Caspase-mediated cleavage of cytoskeletal actin plays a positive role in the process of morphological apoptosis. *Oncogene* **18**, 2423–2430
37. Maciver, S.K. (1996) Myosin II function in non-muscle cells. *Bioessays* **18**, 179–182
38. Mitchison, T.J. and Cramer, L.P. (1996) Actin-based cell motility and cell locomotion. *Cell* **84**, 371–379
39. Rotonda, J., Nicholson, D.W., Fazil, K.M., Gallant, M., Gareau, Y., Labelle, M., Peterson, E.P., Rasper, D.M., Ruel, R., Vaillancourt, J.P., Thornberry, N.A., and Becker, J.W. (1996) The three-dimensional structure of apopain/CPP32, a key mediator of apoptosis. *Nat. Struct. Biol.* **3**, 619–625
40. Mittl, P.R., Di Marco, S., Krebs, J.F., Bai, X., Karanewsky, D.S., Priestle, J.P., Tomaselli, K.J., and Grütter, M.G. (1997) Structure of recombinant human CPP32 in complex with the tetrapeptide acetyl-Asp-Val-Ala-Asp fluoromethyl ketone. *J. Biol. Chem.* **272**, 6539–6547
41. Cohen, C. and Parry, D.A. (1990) α-Helical coiled coils and bundles: how to design an α-helical protein. *Proteins Struct. Funct. Genet.* **7**, 1–15
42. Wei, Q. and Adelstein, R.S. (2000) Conditional expression of a truncated fragment of nonmuscle myosin II-A alters cell shape but not cytokinesis in HeLa cells. *Mol. Biol. Cell* **11**, 3617–3627
43. Nonoguchi, K., Itoh, K., Xue, J.H., Tokuchi, H., Nishiyama, H., Kaneko, Y., Tatsumi, K., Okuno, H., Tomiwa, K., and Fujita, J. (1999) Cloning of human cDNAs for Apg-1 and Apg-2, members of the Hsp110 family, and chromosomal assignment of their genes. *Gene* **237**, 21–28
44. Jäättelä, M., Wissing, D., Kokholm, K., Kallunki, T., and Egeblad, M. (1998) Hsp70 exerts its anti-apoptotic function downstream of caspase-3-like proteases. *EMBO J.* **17**, 6124–6134
45. Robertson, J.D., Datta, K., Biswal, S.S., and Kehrer, J.P. (1999) Heat-shock protein 70 antisense oligomers enhance proteasome inhibitor- induced apoptosis. *Biochem. J.* **344**, 477–485
46. Garrido, C., Bruey, J.M., Fromentin, A., Hammann, A., Arrigo, A.P., and Solary, E. (1999) HSP27 inhibits cytochrome *c*-dependent activation of procaspase-9. *FASEB J.* **13**, 2061–2070
47. Mills, J.C., Stone, N.L., Erhardt, J., and Pittman, R.N. (1998) Apoptotic membrane blebbing is regulated by myosin light chain phosphorylation. *J. Cell Biol.* **140**, 627–636